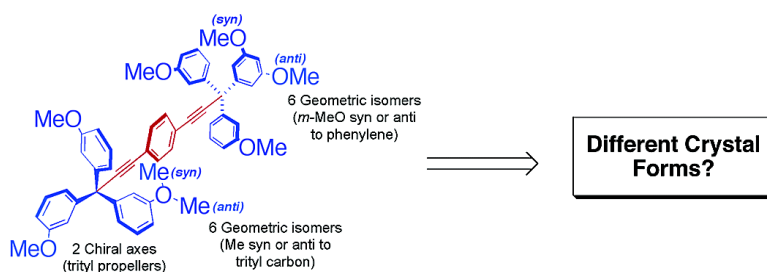


Crystal Phases and Phase Transitions in a Highly Polymorphogenic Solid-State Molecular Gyroscope with *meta*-Methoxytrityl Frames

Jose E. Nuez, Tinh-Alfredo V. Khuong, Luis M. Campos, Norberto Farfn, Hung Dang, Steven D. Karlen, and Miguel A. Garcia-Garibay

Crystal Growth & Design, 2006, 6 (4), 866-873 • DOI: 10.1021/cg050155o

Downloaded from <http://pubs.acs.org> on February 6, 2009



More About This Article

Additional resources and features associated with this article are available within the HTML version:

- Supporting Information
- Links to the 4 articles that cite this article, as of the time of this article download
- Access to high resolution figures
- Links to articles and content related to this article
- Copyright permission to reproduce figures and/or text from this article

[View the Full Text HTML](#)

Crystal Phases and Phase Transitions in a Highly Polymorphogenic Solid-State Molecular Gyroscope with *meta*-Methoxytrityl FramesJose E. Nuñez, Tinh-Alfredo V. Khuong, Luis M. Campos, Norberto Farfán,[‡] Hung Dang, Steven D. Karlen, and Miguel A. Garcia-Garibay*

University of California, Los Angeles, Department of Chemistry and Biochemistry, 405 Hilgard Avenue, Los Angeles, California 90095-1569

Received April 15, 2005; Revised Manuscript Received January 10, 2006

ABSTRACT: The energy landscape of molecular gyroscopes with *meta*-methoxy substituted trityl groups may include many stereoisomers due to the helicity of the two triarylmethyl propeller moieties and the stereochemical label provided by the *meta*-methoxy group. While low equilibration barriers and rapid equilibration in solution prevent isolation and observation by relatively slow techniques such as ¹H and ¹³C NMR, their many structural options may offer opportunities to prepare several crystal forms, or conformational polymorphs. In this paper, we report the synthesis and characterization of 1,4-bis[tri(*meta*-methoxyphenyl)propynyl]benzene (**2**), a crystalline molecular gyroscope with a phenylene rotator, a dialkyne axle, and two tri-*meta*-methoxy-substituted trityl frames. Using a combination of single-crystal X-ray diffraction, differential scanning calorimetry (DSC), thermogravimetric analysis (TGA), high resolution ¹³C cross-polarization magnetic-angle spinning (CPMAS) NMR, and polarized microscopy, we obtained experimental evidence for seven polymorphs labeled A–G and up to six phase transitions that relate them.

Introduction. To prepare solid-state materials built from molecules that emulate the topology and function of macroscopic gyroscopes and compasses (Figure 1), we analyzed structures consisting of a phenylene rotator linked through a barrierless dialkyne axle¹ to shielding triarylmethyl² or triptycyl³ frames. Early results with the parent trityl derivative **1a** (R₁ = R₂ = H, Scheme 1) showed a remarkably fast 2-fold (180°) π -flipping motion in the solid state that emulates the desired gyroscopic motion with exchange rates of ca. 1.6 MHz at ca. 65 °C. Subsequently, we showed that trityl derivative **1b** with bulky *tert*-butyl groups at the two *meta* positions of each phenyl group (R₁ = R₂ = *t*Bu, Scheme 1) reduce the packing density around the central rotator, so that phenylene flipping in the solid state occurred with a rate > 100 MHz at 25 °C.⁴ We have also shown that crystalline molecular compasses with rotating electric dipoles can be interfaced with external electric fields and may be used as artificial dielectric materials.⁵

When structures analogous to those in Figure 1 and Scheme 1 are considered, it is expected that small variations will cause changes in their crystal packing and their rotary dynamics. To establish clear structure–function parameters for rotational dynamics in the solid state, structural and dynamic data from a large number of structures are desired. While variations in solid forms can be introduced by systematic changes at the molecular level attained by synthetic means, the formation of polymorphs^{6,7} and pseudopolymorphs also extends the number of solid-state alternatives for any given structure. Although the preparation of many crystal forms from a given compound by crystallization may sound simple, the formation of polymorphs and pseudopolymorphs is far from trivial. This is highlighted by nonconventional efforts based on polymorph formation by controlled nucleation through epitaxy,⁸ by polymorph growth inhibition with suitable additives,⁹ and by nucleation with another polymorph.¹⁰ In fact, still current, the common wisdom on the subject, as articulated by McCrone in 1963, indicates that “the number of (crystal) forms for a given compound is proportional

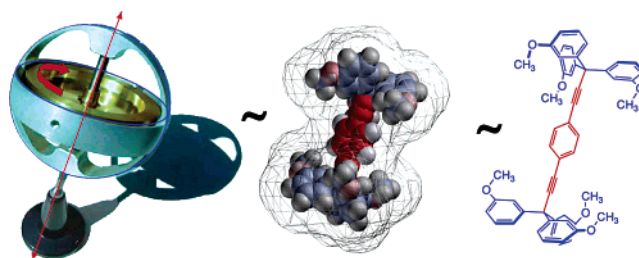
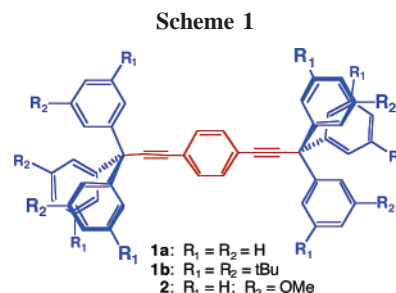


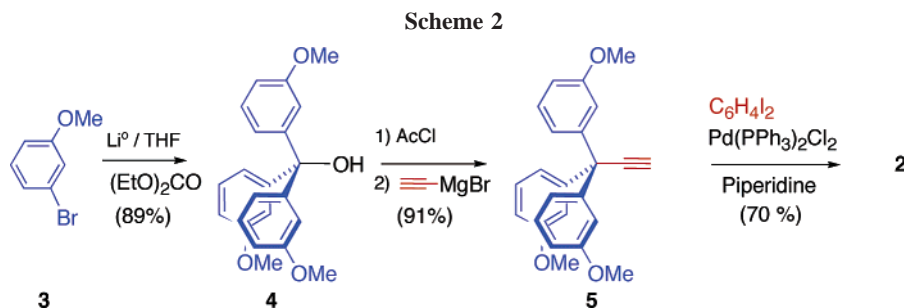
Figure 1. A simple gyroscope consists of a rotator with an axis of rotation that passes through its center of mass and an encapsulating frame that holds the assembly together (left). In the center is a hypothetical solid-state molecular gyroscope showing a phenylene rotator with a dialkyne axis (in red) and an encapsulating frame made up with two tris-*meta*-methoxy-substituted triphenylmethyl groups (in blue). An iconic line formula is shown on the right.



to the time and energy spent in research on that compound.” While the empirical sense conveyed by this quote makes the combinatorial screening of crystallization conditions one of the more promising strategies,¹¹ intuition also suggests that certain structures may be much more polymorphogenic than others. In fact, knowing that crystallization relies on a subtle balance of inter- and intramolecular forces, and that lattice energies of polymorphs differ by ~ 1 – 2 kcal/mol, one may expect that structures with a large number of conformers within a small energy range should be particularly promising.^{12,13} A remarkable illustration of this is the macrocyclic polyether 18-crown-6, which was reported to occur in 54 crystal structures in 12 different conformations.¹⁴ With that in mind, we have prepared

* To whom correspondence should be addressed. E-mail: mgg@chem.ucla.edu.

[‡] Facultad de Química Universidad Nacional Autónoma de México, Ciudad Universitaria, 04510 México D. F., México.



and analyzed 1,4-bis[tri-(*meta*-methoxyphenyl)propynyl]benzene (**2**) ($R = \text{OMe}$, Scheme 1) as a test case. As discussed below, compound **2** is expected to have a remarkably flat conformational landscape with a very large number of energy minima.¹⁵ In agreement with these expectations, a Monte Carlo conformational analysis of 15 000 structures reveals ca. 1600 different structures within 2 kcal/mol, and a modest number of crystallizations from solution followed by temperature variations produced up to seven distinguishable crystal forms. In this paper, we describe the synthesis, crystallization, and solid-state characterization of compound **2** by a combination of single-crystal X-ray diffraction, solid-state cross polarization and magic angle spinning (CPMAS) ¹³C NMR, thermal analyses, and thermal microscopy.

Results and Discussion

Synthesis. The hexamethoxy molecular gyroscope **2** was prepared in three steps from *meta*-bromoanisole **3** as illustrated in Scheme 2. The trityl alcohol **4** was prepared in one step in 89% isolated yield by the reaction of diethyl carbonate with the aryllithium reagent prepared from **3** in THF by metal-halogen exchange. The trityl chloride prepared by the reaction of **4** with acetyl chloride was not isolated but reacted immediately with ethynylmagnesium bromide to give the trityl acetylene **5** in 91% yield. In the final step, two equivalents of the terminal acetylene were submitted to a Pd(0)-coupling reaction with 1,4-diiodobenzene to form compound **2** in 70% yield¹⁶ (Scheme 2). Compound **2** was characterized by conventional spectroscopic methods, and its structure was confirmed by single-crystal X-ray diffraction (see below). The solution ¹H and ¹³C NMR spectra were consistent with a time-averaged symmetric structure. The central phenylene appears in the ¹H NMR as a singlet at 7.43 ppm, with all the trityl aromatics occurring as a set of four coincident signals centered at 7.22, 6.93, 6.88, and 6.80 ppm, and all six methoxy groups as a singlet at 3.74 ppm. The ¹³C NMR consists of eight aromatic carbon resonances between 159.3 and 112.0 ppm, two alkyne signals at 97.1 and 84.9 ppm, and the signals for the two quaternary carbons and six methyl groups at 56.2 and 51.1 ppm, respectively.

Conformational Analysis and Residual Isomerism. To appreciate the number of stereoisomers that may exist at equilibrium in solution, one must consider the conformational preferences and static stereochemistry of triarylmethyl derivatives.¹⁷ It is well-known that the planes of the three rings tend to have a uniform tilt with respect to the $\text{Ar}_3\text{C}-\text{X}$ bond, creating a helical, propeller-like conformation, with either C_1 or C_3 axial symmetry.¹⁸ Structures differing only by the sense of the tilt of the aryl groups are nonsuperimposable mirror images, which, depending on the nature of the three aryl groups and their substituents, may be obtained either as isolable or rapidly interconverting enantiomers (Figure 2a). The spectroscopic data

obtained in solution at ambient temperature and pressure clearly indicate the latter to be true for compound **2**.

In addition to their propeller conformation, triarylmethyl groups in which the aromatic rings lack a local 2-fold symmetry axis coincident with the direction of their $\text{Ar}-\text{C}$ bond display geometric isomers (Figure 2b). In the case of the *meta*-substituted benzenes of compound **2**, this can be easily recognized in terms of the orientation of the MeO substituent (either *syn*- or *anti*-) with respect to the direction of the $\text{Ar}_3\text{C}-\text{CC}\equiv\text{C}$ bond. Finally, as illustrated in Figure 2c, two more geometric stereoisomers are obtained in a given methoxy-substituted aryl group when the direction of the methyl group is considered. Gas phase and computational analysis of simple *meta*-methylanisol and other *meta*-methoxy aromatics indicate the existence of coplanar *syn*- and *anti*-conformers with an energy difference of only ca. 60 cm^{-1} (0.17 kcal/mol).¹⁹ Therefore, the geometric isomers generated by the orientation of each methyl-oxy group with respect to the aromatic ipso-carbon is an additional stereogenic element that increases the number of potential minima in the conformational landscape of **2**.

The relatively flat torsional potentials of the central phenylene and six aryl groups also give rise to nonidentical structures, which may differ only by the magnitude of one or more dihedral angles between the various aromatic planes.²⁰ Even if one ignores this structural aspect and assumes that the trityl groups in **2** will be staggered (see below), one may envision many stereoisomers for the structure (Scheme 3), some of which could

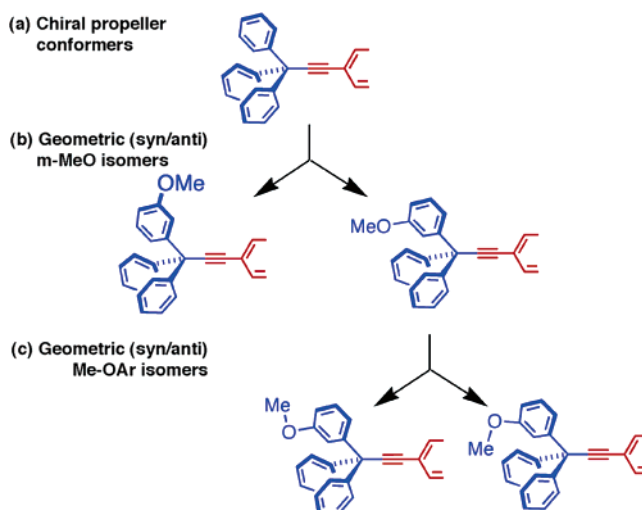
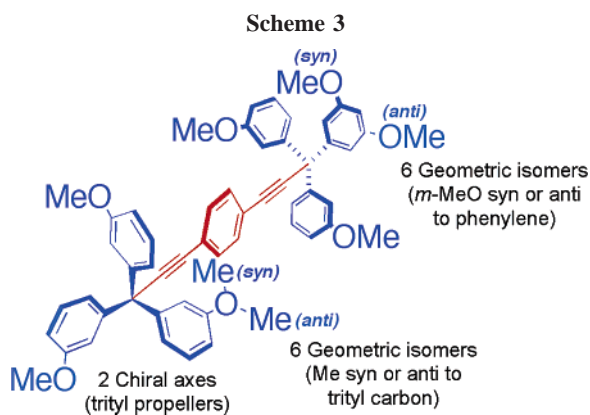


Figure 2. (a) Illustration of the axial chirality with one of the two propeller conformations of a simple triphenylmethyl derivative, (b) geometric isomerism resulting from *meta*-methoxy groups in two different orientations with respect to the phenylethynyl substituent, and (c) geometric isomers arising from the two preferred conformations of the methyl ether with the methyl group pointing toward the *para*- or *ortho*-phenyl carbons.



be isolated in the crystalline state. Notably, with identically substituted trityl groups at the two ends of the structure some of these isomers may have an inversion center, which will render them meso.

Monte Carlo Conformational Search. While gas phase energy variations within this remarkably large structure set are expected to be relatively small, some conformers may experience adverse steric interactions between neighboring methoxy-aryl groups. To confirm the structure of compound **2** and evaluate the number of isomers within ~ 2 kcal/mol, we carried out a systematic Monte Carlo multiple minimum (MCMM)²¹ conformational search, using the AMBER force field.²² To mimic our crystallographic results (see below), we assumed the relation between trityl groups to be staggered and investigated a number of different conformations within a range of convergent root-mean-square deviation values of cRMS = 0.25 Å and cRMS = 1.5 Å. The cRMS deviation is the norm of the distance vector between two sets of atomic coordinates that have been optimally superimposed and is a common measure of structural similarity.²¹ Values in the studies range were analyzed to establish criteria to reject structures that differ by small variations in the tilt of the aromatic rings of the trityl groups. As expected, the total number of different structures identified for a given number of Monte Carlo searches decreased with this structural restriction and essentially converged between cRMS = 1.0 Å and cRMS = 1.5 Å. The total number of (different) structures within a given energy window was also analyzed for convergence as a function of the total number of structures searched. Sample sizes of 1000, 5000, and 15 000 provided 427, 1136, and 1608 energy minima within 2.0 kcal/mol for a cRMS = 1.5 Å limit, and as many as 740, 2700, and 4641 for those sample sizes when the energy window was increased to 5 kcal/mol. Notably, the global energy minimum found in all these calculations was consistent with a conformation that has two of the three methoxy groups on each trityl syn- to the phenylene, and all the methyl ether groups in each of the six phenyls directed to their corresponding ortho-carbon. From the conformational search sampling 15 000 structures, the conformation of highest energy within a 5 kcal/mol range has all the methoxy groups syn to central phenylene and all methyl groups directed to the *para*-phenyl carbon. Interestingly, analysis of a few random structures suggest no obvious adverse steric effects, suggesting that polar interactions may determine the energy differences between the structures in this set.

X-ray Analysis. In search of solid phases containing different conformations of compound **2**, we carried out a relatively small number of crystallizations from several common solvents and solvent mixtures, including chloroform, dichloromethane, acetone, diethyl ether, hexane, dichloroethane, dimethoxyethane, and benzene. Distinct X-ray quality crystals were obtained by

slow evaporation from benzene (25 °C) and dichloromethane (25 °C, -10 °C). The former were characterized as a benzene clathrate, which is a crystal form with “incarcerated” benzene²³ [form **A**], and the latter as a solvent-free structure [form **B**, 25 °C] and a dichloromethane clathrate [form **G**, -10 °C]. X-ray quality crystals grown from acetone, 1,2-dimethoxyethane, hexanes, and acetonitrile at 25 °C had cell dimensions identical to those of phase **B**, but the heterogeneous appearance of those samples suggested additional crystal forms (see below). Given that solid forms **A** and **B** have different compositions due to the solvent of crystallization, they are formally considered pseudopolymorphs rather than polymorphs. We noticed that crystallization from solvents (dichloromethane, acetone, hexane, etc., 25 °C) containing minute amounts of benzene had a strong tendency to form clathrate **A**, and that forms **A** and **B** sometimes occurred concomitantly under those conditions.²⁴ Although no other forms suitable for single-crystal X-ray analysis were apparent from solution crystallization at ambient temperature, three other forms (**C–E**) were discovered upon heating samples of **A** and **B** (see below) and two more (**F** and **G**) by crystallization at low temperatures. From the latter, solvent-containing samples of form **G** crystallized at -10 °C from dichloromethane. These crystals were suitable for single-crystal X-ray diffraction, and their structure was determined along with those of **A** and **B**. Key crystallographic data for the two pseudopolymorphs **A** and **B**, and polymorph **G**, are included in Table 1. Notably, all three structures are centrosymmetric with coincident crystallographic and molecular inversion centers. The structure of the solvent-free crystal (**B**) was solved in the monoclinic space group $P2_1/c$ with half a molecule per asymmetric unit and two molecules per unit cell. The structures of the benzene clathrate (**A**) and the dichloromethane clathrate (**G**) were solved in the triclinic space group $P\bar{1}$ with half a molecule of **2** and one molecule of solvent per asymmetric unit. As expected from our conformational analysis, the molecular structures determined in the three crystal forms represent different conformational isomers.

An ORTEP representation of the molecular structure of form **A** (collected at 100 K, thermal ellipsoids drawn at 50% probability level) is shown in Figure 3a along with a packing diagram illustrating its unit cell and one benzene molecule at the center of the unit cell. With the trityl groups adopting asymmetric C_1 conformations of opposite chirality, the molecular structure is meso. With respect to the center of the molecule, two methoxy groups (C25 and C26) are anti, and one (C27) is syn. All of them have methyl groups directed toward the *para*-carbon. This conformation gives rise to a large cavity that accommodates the caged benzene molecule, which can be clearly appreciated at the center of the unit cell in Figure 3a. Notably, the benzene clathrate **A** differs from those observed with the parent compound **1a**² and several of its phenylene-substituted derivatives.²⁵ While benzene molecules in those clathrates occur as parallel-displaced dimers, the structure of **A** contains only one benzene molecule in the center of the unit cell (Figure 3a). The packing structure of **A** is characterized by having all molecules in a parallel alignment with several sp^2 CH \cdots O and sp^3 CH \cdots O interactions, with the shortest two being only 2.44 and 2.55 Å.

An ORTEP diagram of form **B** drawn at the 50% probability level in Figure 3b (acquired at 298 K) shows all six methoxy substituents in a syn-conformation pointing toward the central phenylene ring. As in form **A**, the local symmetry of the trityl groups is C_1 , but the centrosymmetric molecular structure is meso. Two methyl groups (C26 and C27) are oriented toward the *para*-phenyl carbon and the third (C25) toward the ortho

Table 1. Principal Crystallographic Parameters for the Hexa-(*meta*-methoxy-triphenylmethyl) Derivatives of 1,4-Bis-(3,3,3-triphenylpropynyl)Benzene [A, B, and G]^a

	C ₅₄ H ₄₆ O ₆ ·C ₆ H ₆ (A)	C ₅₄ H ₄₆ O ₆ (B)	C ₅₄ H ₄₆ O ₆ ·2(CH ₂ Cl ₂) (G)
empirical formula	C ₅₄ H ₄₆ O ₆ ·C ₆ H ₆ (A)	C ₅₄ H ₄₆ O ₆ (B)	C ₅₄ H ₄₆ O ₆ ·2(CH ₂ Cl ₂) (G)
formula weight	869.02	790.91	960.76
crystal system	triclinic	monoclinic	triclinic
space group	<i>P</i> 1̄	<i>P</i> 2 ₁ / <i>c</i>	<i>P</i> 1̄
<i>Z</i>	1	2	1
size, mm ³	0.35 × 0.20 × 0.10	0.62 × 0.60 × 0.52	0.40 × 0.20 × 0.20
color, morphology ^a	prisms	prisms	parallelepiped
temperature, K	100(2)	298(2)	120(2)
unit cell dimensions			
<i>a</i> , Å	6.9849(10)	11.834(2)	8.906(2)
<i>b</i> , Å	10.1656(15)	11.931(2)	11.926(3)
<i>c</i> , Å	17.697(3)	15.764(3)	11.959(3)
<i>a</i> , deg	77.320(2)	90	89.392(4)
<i>b</i> , deg	82.054(2)	105.390(3)	73.078(4)
<i>g</i> , deg	73.833(2)	90	89.372(4)
<i>V</i> , Å ³	1173.4(3)	2146.0(6)	1215.1(5)
<i>D</i> _c , Mg/m ³	1.230	1.224	1.313
total reflections	10321	18841	9823
independent reflections	5423	5196	4936
	[R(int) = 0.0446]	[R(int) = 0.0200]	[R(int) = 0.0416]
R1 [<i>I</i> > 2σ(<i>I</i>)]	0.0611	0.0443	0.0596
wR2 (all data)	0.1753	0.1312	0.1380

^a Crystals grown from benzene (25 °C) for **A**, dichloromethane (25 °C) for **B**, and from dichloromethane (−10 °C) for **G**.

position. A slight curvature along the axis of the alkyne triple bonds is seen in the structure, with C4 and C5 bending out of an imaginary line drawn between C3 and C6. The distortion in the alkyne bonds is further illustrated in the packing arrangement in Figure 3b, as molecules adopt a slight *S*-conformation with the trityl groups of adjacent molecules making close contacts. Not evident in Figure 3b is the layer of molecules with their long axes making an angle of 65.69° with respect to that the molecules shown.

The ORTEP representation and unit cell arrangement of structure **G** are shown in Figure 3c, at 50% probability, acquired at 120 K. This structure was solved in the triclinic space group *P*1̄ with half a molecule of 2 and one of CH₂Cl₂ per asymmetric unit. This structure is also meso, with the trityl groups in *C*₁ conformations and all methoxy substituents arranged in a syn-conformation to the dialkyne axis. The methyl groups labeled C26 and C27 are directed toward the ortho-carbon and the third one, C25, is directed toward the *para*-position. Several edge-to-face interactions between the trityl groups of adjacent molecules and an sp² CH···O interaction between H(2) of the central phenylene and O(3) in one of the methoxy groups, at a distance of 2.59 Å, are notable in the structure. Dichloromethane molecules occur in pairs related by an inversion center with no close contacts between them within a cage structure formed by four molecular gyroscopes. Close contacts involving the dichloromethane hydrogens include interactions with one of the neighboring methoxy oxygens, at a distance of 2.435 Å [Cl₂HC–H(2S)···O(1)]. The second hydrogen has contacts with carbons in the aromatic ring of one the neighboring phenyl groups with distances of 2.68 Å [Cl₂HC–H(1S)···C(19)] and 2.273 Å [Cl₂HC–H(1S)···C(20)]. As the other structures, a small curvature along the alkyne axis can also be appreciated when one traces a line between the ipso and triarylmethyl carbons C3–C6.

Solid Phases and Phase Transitions. An initial determination of the melting points of forms **A** and **B**, with finely ground samples in a capillary tube using a slow heating rate revealed identical, sharp melting points at 181 °C, suggesting that form **A** loses benzene to give form **B** in an apparent solid-to-solid transformation. Thermogravimetric analysis of form **A** confirmed the loss of mass corresponding to one molecule of benzene at 135–140 °C. However, while searching for a confirmation of the melting point observations by DSC with

experiments run at 2–10° min^{−1} with forms **A** and **B** we detected several small peaks in addition to the melting endotherm at 181 °C (Figure 4). It was later shown that the latter melting transition corresponds to a daughter phase subsequently labeled as phase **D** (please see below).

DSC experiments with clathrate **A** and solvent-free crystals **B** at various heating rates revealed a complex behavior (Figure 4). At least five different phases (**A**–**E**) were deduced from endothermic transitions with intensities that depended on heating rates and whether the samples were allowed to equilibrate between consecutive transitions. Three representative runs are shown in Figure 4. The top trace is from a DSC experiment run at a rate of 10° min^{−1} that started with the solvent-free phase **B** grown from dichloromethane. The middle and bottom traces are from experiments with the benzene clathrate **A** at rates of 10° min^{−1} and 5° min^{−1}, respectively. The sample in the bottom trace was allowed to equilibrate for 20 min at 145 and 160 °C with the intention of annealing the phases that form at 141 and 153 °C, respectively. The melting transition previously observed in melting point experiments at 181 °C was named **D**. In agreement with the slow heating visual observations, the intensity of this transition increased in size with decreasing heating rates and was the largest peak at 2° min^{−1}, (not shown), suggesting that it may be thermodynamically the most stable phase. Experiments with freshly crystallized samples heated just past each of the observed transitions, cooled to ambient temperature, and subsequently heated to the same temperature showed all of them to be thermally irreversible. From all five transitions, only the endotherm assigned to the melting of phase **E** at 173 °C was always small and irreproducible. In no case was crystallization from the melt observed after samples had been heated beyond 181 °C. A relation between the heating rate and the intensity of the endotherm from **B** to **C**, and from **D** to the melt, suggests that phase **C** may be formed under kinetic control (upon fast heating), while phase **D** may form preferentially under thermodynamic control (slow heating).^{10,26}

Searching for conditions that might reveal new phases, we carried out DSC analysis of several samples obtained by crystallization from various solvents, at ambient temperature, in a freezer kept at −10 °C, and in a dry ice/acetone bath at −78 °C. Microcrystals obtained from 1,2-dimethoxyethane and 1,2-dichloroethane at 25 °C were analyzed by DSC, giving large endotherms corresponding to phase **C**. DSC runs with crystals

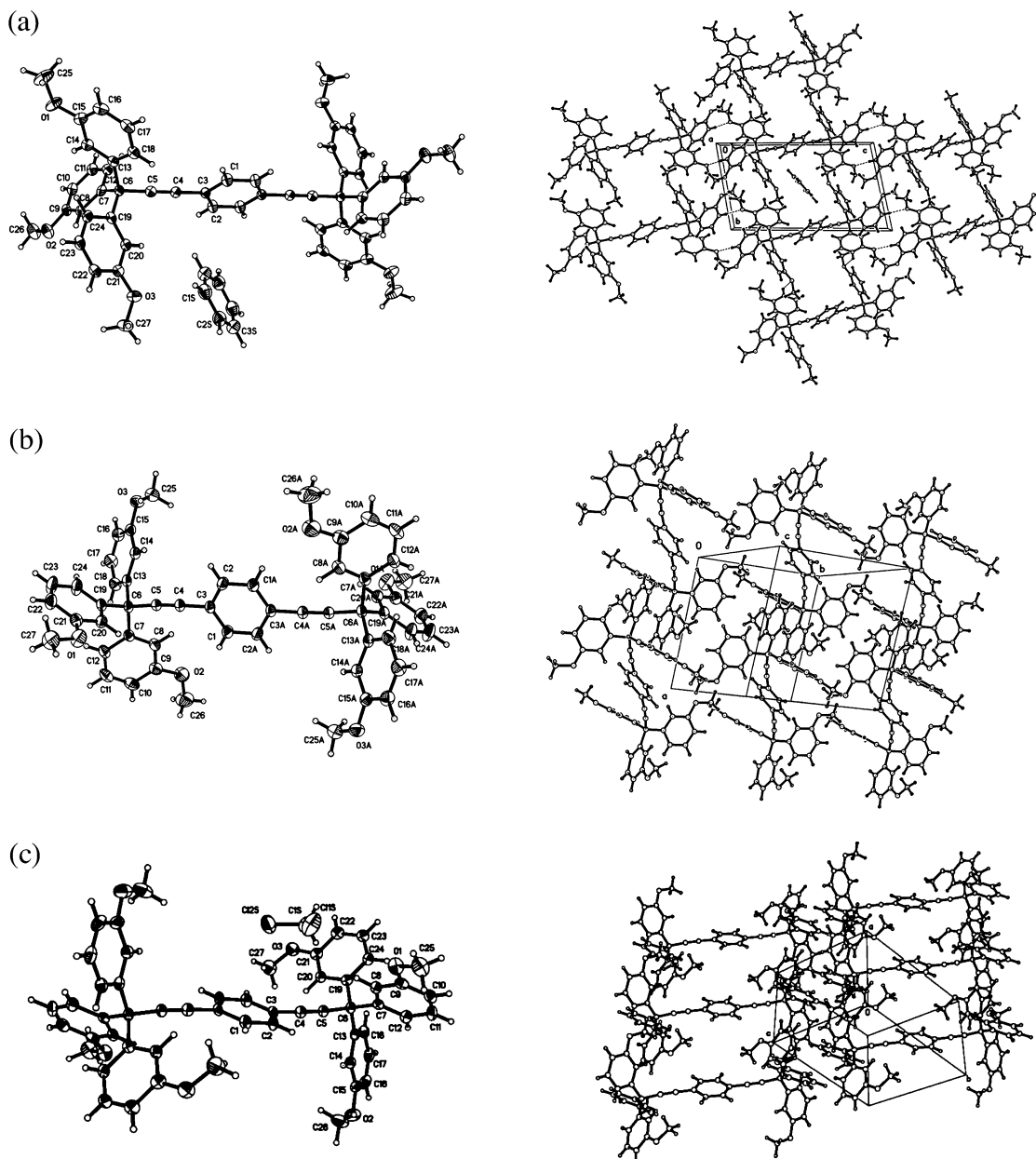


Figure 3. (Left) ORTEP and (right) packing diagrams of (a) the benzene clathrate of molecular gyroscope **2** (form **A**). (b) Solvent-free form of **2** (form **B**). (c) Dichloromethane clathrate of **2** (form **G**).

grown from acetone at ≤ -10 °C showed a small exothermic transition at 138 °C that was followed by the melting transition of phases **C** and **D**. This new phase was not suitable for single-crystal X-ray diffraction and was designated with the letter **F**. Crystallization from dichloromethane at -10 °C afforded phase **G**, which loses solvent over a broad temperature range, followed by a small exothermic transition at 134 °C as these convert to phase **C**, which was characterized by its melting point at 167 °C.

Thermal Microscopy. Variations in the endotherm intensity of consecutive thermal transitions observed in different experiments suggested that not all the phases present in these experiments are always formed in a sequential manner. Therefore, to help us understand the results from the DSC experiments, we carried out visual observations as a function of temperature with a polarizing microscope. A model consistent with all thermal analysis and microscopic observations is depicted in Scheme 4. Although samples grown from benzene and dichloromethane appeared homogeneous by macroscopic

examination and spectral analysis (see below), the presence of small amounts of additional phases, which may later act as seeds, cannot be rigorously discarded. Starting with samples of form **A** grown from benzene with a heating rate of $10^{\circ} \text{min}^{-1}$ we were able to observe the loss of solvent (efflorescence) as form **A** transforms into form **B**. A selection of photomicrographs taken between ca. 30 and 182 °C are available in PDF format as Supporting Information. Crystals of **A** appeared mainly as thin plates and thin plate conglomerates, although a few appeared as prisms. Solvent efflorescence and the onset of opacity started sharply at ca. 141 °C for all the crystals in the view. As the temperature increased to 149–152 °C, about half to two-thirds of all crystals in the view melted while the rest remained apparently unchanged. Differences in the thermal behavior of different specimens may be taken as an indication of nucleation and growth of different daughter phases from the same mother phase.^{10,26} Since the same behavior was observed with samples of phase **A** by in situ desolvation, and with samples of phase **B** obtained by crystallization from dichloromethane

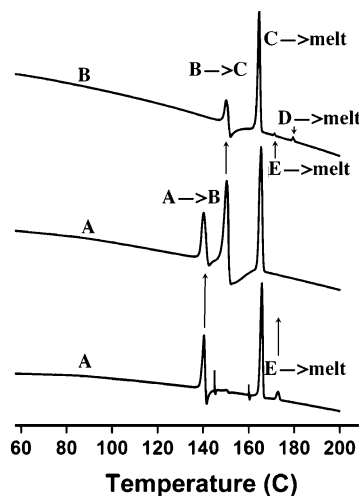


Figure 4. DSC traces (endothermic transitions upward) illustrating the phase transitions of molecular gyroscope **2**. Top: starting from the solvent-free form **B** at a heating rate of $10^\circ \text{ min}^{-1}$. Middle: starting from benzene clathrate form **A** at a heating rate of $10^\circ \text{ min}^{-1}$. Bottom: starting from benzene clathrate **A** at 5° min^{-1} and pausing for 20 min at 145 and 160 $^\circ\text{C}$.

(25 $^\circ\text{C}$), one may assign **B** as the mother phase of phases **C** and **D** (and probably **E**). A metastable liquid formed from phase **B** at 151 $^\circ\text{C}$, which began to crystallize almost immediately, at 153 $^\circ\text{C}$, gave rise to a new transient solid that subsequently melted at 167 $^\circ\text{C}$. We assign these transitions, indicated on the right sidearm of the flowchart in Scheme 4, to the formation and melting of phase **C**. Finally, the fraction of the sample that remained solid started to melt at 179 $^\circ\text{C}$ and turned completely isotropic at 181 $^\circ\text{C}$, allowing us to assign it to phase **D**. In contrast to some of the DSC experiments where a small melting transition was observed at 173 $^\circ\text{C}$, there were no visual microscopic changes that could be correlated with the melting of phase **E**.

Solid-State CPMAS ^{13}C NMR Analysis. In search of additional information on crystal phases **A–E**, ^{13}C CPMAS NMR spectra were acquired in experiments carried out by heating freshly prepared samples in 5–10 degree increments from 100 to 190 $^\circ\text{C}$, allowing them to equilibrate for 30 min, and cooling them down to ambient temperature to record their spectra. These experiments mirror the slow heating (i.e., 2°

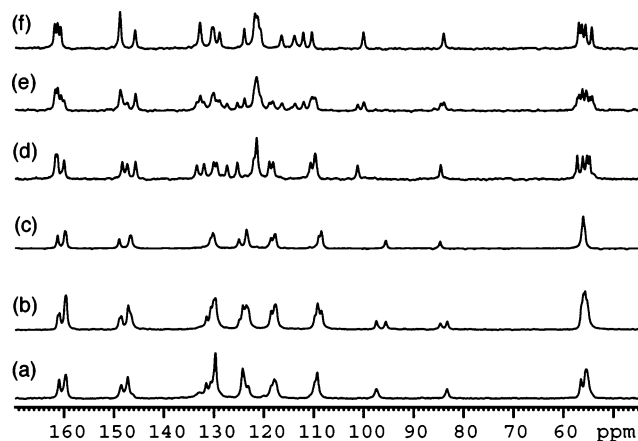
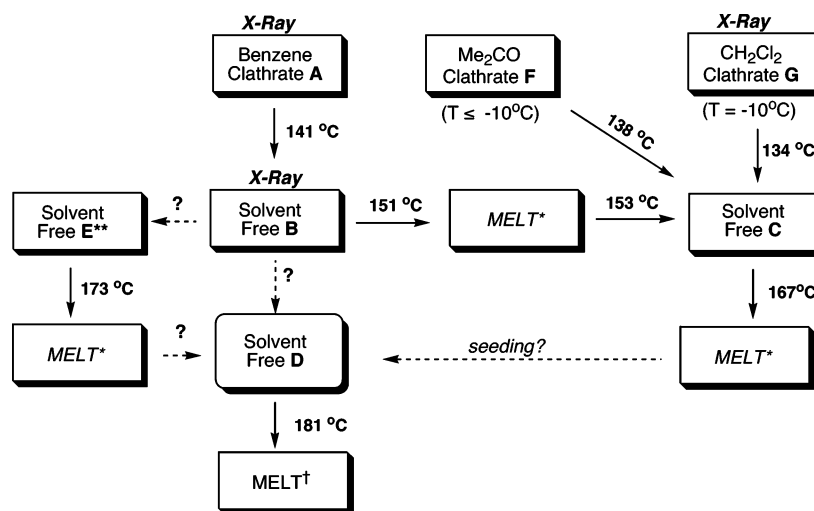


Figure 5. Solid-state CPMAS ^{13}C NMR spectra of **2** taken at 298 K after having exposed the sample for 30 min periods to reduced pressure (10^{-3} Torr), or ca. 10 degree temperature increments, until the change was complete: (a) Samples freshly crystallized from benzene remained unchanged for no less than a week at 298 K (phase **A**). (b) Some desolvation occurs after exposure to 10^{-3} Torr for 6 h (phases **A** and **B**). (c) Pure phase **B** was obtained after heating phase **A** to 135 $^\circ\text{C}$ for 60 min. This spectrum was identical to that obtained with crystals grown from dichloromethane (25 $^\circ\text{C}$). (d) Phase **C** is obtained after heating to 153 $^\circ\text{C}$ for a total of 3 h. (e) Phases **C** and **D** can be detected after heating 160 $^\circ\text{C}$ for a total of 3 h. (f) Pure phase **D** after heating to 160 $^\circ\text{C}$ for a total of 12 h. No changes corresponding to phase **E** were observed and melting occurred 180 $^\circ\text{C}$. The spectrum obtained after melting consisted of very broad peaks as expected for an amorphous glass.

min^{-1}) DSC runs and visual melting observations on capillary tubes, where no liquid phases were observable (presumably due to self-seeding). At the beginning of the experiment, the thermal stability of phase **A** at ambient temperature and its relatively slow desolvation under reduced pressure were documented. After certain heating periods, when the spectrum revealed two distinguishable phases, the sample was allowed to remain at the same temperature until the transformation had been completed. The results summarized in Figure 5 confirm the remarkable homogeneity of phase **A** suggested by the DSC results and reveal four of the five postulated phases. Clear differences were observed in spectra obtained before and after heating to 135 $^\circ\text{C}$ (Figure 5, spectrum c), 153 $^\circ\text{C}$ (spectrum d), and 160 $^\circ\text{C}$ (spectrum f). No changes were observed after

Scheme 4^a



^a *Metastable liquids recrystallize spontaneously and/or by seeding. **Phase **E** only detected by DSC. †The final melt forms a glass upon cooling.

heating beyond 167 °C or until melting, confirming the visual observations with the polarizing microscope. A spectrum obtained after the sample reached the stable liquid at 181 °C (not shown) was extremely broad, as expected for an amorphous material composed of a large number of structures trapped by the highly viscous medium.

Two of the most notable changes in the ^{13}C NMR spectra of the various solid phases are the significant shifting of the two alkyne peaks (between 82 and 110 ppm) and the progressively lower symmetry with increasing phase formation temperature, as judged by the increasing number of peaks across the spectra. The spectra from phases **A** and **B** are relatively simple. Although they have three crystallographic and magnetically nonequivalent methoxy groups (between 50 and 60 ppm), their spectra have a nonresolved peak, which overlaps partially (**A**), or completely (**B**), with the quaternary "methane" carbon. Although there are clear variations in the chemical shift of the alkyne carbons of phases **A** and **B**, probably due to field effects from the benzene molecule in **A** and the different alignment of the oxygen ethers lone pairs in both, all the aromatic signals are remarkably coincident. In contrast, variations in the aromatic signals in going from these two phases to phases **C** and **D** are quite remarkable (between 108 and 165 ppm). Although phases **C** and **D** could represent different packing arrangements of the conformers present in **A** and **B**, their chemical shift dispersion is unlikely to arise from field effects due to different packing arrangements and are more likely to reflect different conformations. Although they both have three methoxy signals, a methane carbon, and up to 16 aromatic signals clearly distinguishable, the presence of only two alkyne carbons strongly suggests internal symmetry between the two trityl sides, just as in phases **A** and **B**. However, the chemical shift dispersion and relatively large number of aromatic signals in the spectra of phases **C** and **D** suggest structures of low symmetry, making it interesting to speculate on the possible formation of chiral crystals by spontaneous resolution of molecules adopting disymmetric point groups.

Conclusions. The structural diversity available to molecular gyroscope **2** is nicely manifested in the solid state in terms of a relatively rich conformational isomerism accompanied by solvent clathrate formation and phase transitions. Clear spectroscopic, calorimetric, and microscopic evidence were obtained for seven distinct phases labeled **A–G**. Experiments run with phase **A** using a very slow heating rate proceeded with no apparent liquid phases and allowed for the selective preparation of phases **B–D**, which could be characterized by solid-state ^{13}C CPMAS NMR. Phase **B** could be obtained by slow solvent evaporation from dichloromethane or by a solid-to-solid-phase transition and loss of benzene from clathrate **A**. Experiments run with fast heating rates revealed the formation of phase **C** by melting and recrystallization of phase **B**. While there were no microscopic observations indicating the formation of phases **D** and **E**, DSC analyses suggest that they may form directly from phase **B**. However, nucleation of one or more phases by another phase should not be discounted.^{10,26} Finally, while many polymorphs may be obtained with significant effort from any given compound, molecular compass **2** easily provided us with at least seven different phases with potentially different gyroscopic dynamics to be analyzed soon. Studies in progress are now aimed at the preparation of molecular gyroscopes with substituents having a chiral center, which will increase the number of possible structures, and which, when resolved, may influence the configurations of the axial and planar chirality of the highly polymorphogenic *meta*-alkoxy substituted trityl groups.

Acknowledgment. This work was supported by the National Science Foundation through Grants DMR-0307028, DMR-9975975 (Solid State NMR), and NSF IGERT: Materials Creation Training Program (Grant No. DGE-0114443). Support from NSF, Paul & Daisy Soros (L.M.C.), and UC-Mexus (N.F.) Fellowships are gratefully acknowledged. We also thank Prof. K. N. Houk for computer use.

Supporting Information Available: Synthesis and spectroscopic characterization of compounds **4**, **5**, and **2**; crystallographic information files (CIF) of forms **A**, **B**, and **G**; microscopic observations illustrating phase changes as a function of temperature. This material is available free of charge via the Internet at <http://pubs.acs.org>.

References

- (1) (a) Saebo, S.; Almolof, J.; Boggs, J. E.; Stark, J. G. *J. Mol. Struct. (THEOCHEM)* **1989**, *59*, 361–373. (b) Abramov, A. V.; Almenningen, A. Cyvin, B. N.; Cyvin, S. J.; Jonvik, T.; Khaikin, L. S.; Rommingin, C.; Vilkov, L. V. *Acta Chem. Scand.* **1988**, *A42*, 674–678. (c) Sipachev, V. A.; Khaikin, L. S.; Grikin, O. E.; Nikitin, V. S.; Traettberg, M. *J. Mol. Struct.* **2000**, *523*, 1–22. (d) Seminario, J.; Zacarias, A. G.; Tour, J. M. *J. Am. Chem. Soc.* **2000**, *122*, 3015–3020. (e) Miteva, T.; Palmer, L.; Kloppenburg, L.; Neher, D.; Bunz, U. H. F. *Macromolecules* **2000**, *33*, 652–654.
- (2) (a) Dominguez, Z.; Dang, H.; Strouse, M. J.; Garcia-Garibay, M. A. *J. Am. Chem. Soc.* **2002**, *124*, 2398–2399. (b) Dominguez, Z.; Dang, H.; Strouse, M. J.; Garcia-Garibay, M. A. *J. Am. Chem. Soc.* **2002**, *124*, 7719–7727.
- (3) (a) Godinez, C. E.; Zepeda, G.; Garcia-Garibay, M. A. *J. Am. Chem. Soc.* **2002**, *124*, 4701–4707. (b) Godinez, C. E.; Zepeda, G.; Garcia-Garibay, M. A. *J. Am. Chem. Soc.* **2002**, *124*, 4701–4707.
- (4) Khuong, T.-A. V.; Zepeda, L. G.; Ruiz, R.; Khan, S. I.; Garcia-Garibay, M. A. *Cryst. Growth Des.* **2004**, *4*, 15–18.
- (5) Horansky, Robert D.; Clarke, Laura I.; Price, John C.; Khuong, Tinh-Alfredo V.; Jarowski, Peter D.; Garcia-Garibay, Miguel A. *Phys. Rev. B.* **2005**, *72*, 014302.
- (6) McCrone, W. C. In *Physics and Chemistry of the Organic Solid State*; Fox, D., Labes, M. M., Wesseberger, A., Eds.; John Wiley & Sons: New York, 1963; Vol. 1; p 725.
- (7) Giron, D. *Thermochim. Acta* **1995**, *248*, 1–59.
- (8) Mitchell, C. A.; Yu, L.; Ward, M. D. *J. Am. Chem. Soc.* **2001**, *123*, 10830–10839.
- (9) (a) Weissbuch, I.; Leiserowitz, L.; Lahav, M. *Adv. Mater.* **1994**, *6*, 952–956. (b) Davey, R. J.; Blagden, N.; Potts, G. D.; Dochery, R. *J. Am. Chem. Soc.* **1997**, *119*, 1767–1772.
- (10) Yu, L. *J. Am. Chem. Soc.* **2003**, *125*, 6380–6381.
- (11) Morissette, S. L.; Almarsson, O.; Peterson, M. L.; Remenar, J. F.; Read, M. J.; Lemmo, A. V.; Ellis, S.; Cima, M. J.; Gardner, C. R. *Adv. Drug Delivery Rev.* **2004**, *56*, 275–300.
- (12) Bernstein, J. *Polymorphism in Organic Chemistry*; Oxford University Press: Oxford, 2002.
- (13) Corradini, P. *Chem. Ind.* **1973**, *55*, 122–129.
- (14) Dobler, M. *Chimia* **1984**, *38*, 415–421.
- (15) Eliel, E. L.; Wilen, S. H. *Stereochemistry of Organic Compounds*; John Wiley & Sons: New York, 1994.
- (16) (a) Pearce, P. J.; Richards, D. H.; Scilly, N. F. *J. Chem. Soc., Perkin Trans. 1* **1972**, 1655–1660. (b) Raker, J.; Glass, T. E. *Tetrahedron* **2001**, *57*, 10233–10240. (c) Feldman, K. S.; Weinreb, C. K.; Youngs, W. J.; Bradshaw J. D. *J. Am. Chem. Soc.* **1994**, *116*, 9019–9026.
- (17) (a) Mislow, K. *Acc. Chem. Res.* **1976**, *9*, 26–33. (b) Mislow, K.; Gust, D.; Finocchiaro, P.; Boettcher, R. J. *Top. Curr. Chem.* **1974**, *47*, 1–28.
- (18) (a) Finocchiaro, P.; Gust, D.; Mislow, K. *J. Am. Chem. Soc.* **1973**, *95*, 8172–8173. (b) Hayes, K. S.; Nagumo, M.; Blount, J. F.; Mislow, K. *J. Am. Chem. Soc.* **1980**, *102*, 2773–2776.
- (19) (a) Breen, P. J.; Bernstein, E. R.; Secor, H. V.; Seeman, J. I. *J. Am. Chem. Soc.* **1989**, *111*, 1958–1968. (b) Ichimura, T.; Suzuki, T. *J. Photochem. Photobiol. C: Photochem. Rev.* **2000**, *1*, 79–107.
- (20) For very rich polymorphism accompanied by changes on the soft torsion potential of phenyl groups see Kumar, V. S. S.; Adlagata, A.; Nangia, A.; Robinson, W. T.; Broder, C. K.; Mondal, R.; Evans, I. R.; Howard, J. A. K.; Alen, F. H. *Angew. Chem., Int. Ed.* **2002**, *41*, 3848–3851.
- (21) Mohamadi, F.; Richards, N. G. J.; Guida, W. C.; Liskamp, R.; Lipton, M.; Caufield, C.; Chang, G.; Hendrickson, T.; Still, W. C. *J. Comput. Chem.* **1990**, *11*, 440–467.

- (22) (a) Weiner, S. J.; Kollman, P. A.; Case, D. A.; Singh, V. C.; Ghio, C.; Alagona, G.; S. Profeta, J.; Weinre, P. *J. Am. Chem. Soc.* **1984**, *106*, 765–784. (b) Calculations were performed using the Maestro 3.0.338 package (Schrodinger, Portland, OR).
- (23) McNicol, D. D.; Toda, F.; Bishop, R. *Comprehensive Supramolecular Chemistry*; Pergamon: Oxford, 1996; Vol. 6.
- (24) Two or more crystal forms of a given compound that occur simultaneously under a given set of experimental conditions are referred to as concomitant polymorphs: Bernstein, J.; Davey, R. J.; Henck, J.-O. *Angew. Chem., Int. Ed. Engl.* **1999**, *38*, 3441–3461.
- (25) Dominguez, Z.; Khuong, T.-A. V.; Dang, H.; Sanrame, C. N.; Nuñez, J. E.; Garcia-Garibay, M. A. *J. Am. Chem. Soc.* **2003**, *125*, 8827–8837.
- (26) Yu, Y. *Cryst. Growth Des.* **2003**, *3*, 967–971.

CG050155O